MALIGNANT TUMOR DETECTION USING FINITE VOLUME TIME DOMAIN

K. O. Dinga[1], D. B.O Konditi[2] and H. Ouma[3]
[1]Department of Electrical Engineering, Jomo Kenyatta University of Agriculture and Technology, Nairobi, Kenya
[2]Faculty of Engineering, Multi-Media University College of Kenya, Nairobi, Kenya
[3]School of Engineering, University of Nairobi, Nairobi Kenya

Abstract
For a long time microwave engineers have dreamed of using non-ionizing electromagnetic waves to image the human body in order to detect cancer. Over the past several years, significant progress has been made towards making this dream a reality for breast cancer detection. In the next decade, microwave systems are likely to become viable diagnostic option for many women and men alike. More so than for any other cancers, breast tumors have electrical properties at microwave frequencies that are significantly different from those of healthy breast tissues. The breast can easily be accessed from outside, while internal organs are much less accessible. Normal breast tissue is also more translucent to microwaves than many other tissues, such as muscle or brain. Phenomenal progress in computers and numerical techniques during the past decade allows us to effectively process data acquired through measurements. This work proposes a new methodology for analyzing malignant tumors. The methodology will be based on finite volume time domain (FVTD) modeling approach. In the past finite difference time domain modeling schemes have been used to detect tumors. However, though it is simple and has wide frequency coverage, its main drawback is that it is computationally intensive. To overcome this drawback finite volume time domain (FVTD) is proposed as a suitable modeling technique for the problem.

Key words: Conformal microwave technology, finite difference time domain, malignant tumor, permittivity, conductivity, finite volume time domain

1.0 Introduction

There is considerable recent debate as to whether or not women under 50 years of age should have X-ray mammograms. This debate arises from the need to detect breast cancer in its earliest stage. Early detection leads to longest survival and greatest patient comfort. While mammography is recognized as the preferred method to detect breast cancer, it fails to detect as many as 20% of the malignant tumors. Further, it may be uncomfortable or threatening to many of the patients, especially with the public perception that repeated X-ray mammograms increase the risk of cancer. Other modalities such as ultrasound and magnetic resonance imaging (MRI) are either less effective or too costly. Pulsed confocal microwave technology can complement mammography by remedying most of the above noted deficiencies.

1.1 Physical Basis of the Method

The confocal, microwave breast cancer detection technology is based upon two fundamental properties of breast tissues at microwave frequencies. Microwaves interact with biological tissues primarily according to the tissue water content. This is a different interaction mechanism than for X-rays. The relevant physical properties contrast between malignant tumors and normal breast tissues is significantly greater for microwaves than for either X-rays or ultrasound, approaching an order of magnitude. This large dielectric contrast causes malignant tumors to have significantly greater microwave scattering cross sections than normal tissues of comparable geometry.

Microwave attenuation in normal breast tissue is less than 4 dB/cm up to 10 GHz. This may permit existing microwave equipment having standard sensitivity and dynamic range to detect tumors located up to about 5 cm beneath the skin. The microwave attenuation and phase characteristic of normal breast tissue is such that constructive addition is possible for wide-bandwidth backscattered returns using broad aperture confocal-imaging techniques. The confocal technique suppresses returns from spurious scatterers such as a vein interposed between the tumor and the surface of the breast.

1.2 Breast Tissue Dielectric Properties

Dielectric Contrast between Malignant Tumors and Surrounding Normal Breast Tissue

Measurements of 30 different tissue types by Gabriel *et al.* [1]–[4] indicate that the relative dielectric permittivity ε_r, and conductivity σ, of high-water-content tissues (such as muscle or malignant tumors) are about an order of magnitude greater than those of low-water-content tissues (such as fat or normal breast tissue). As illustrated in figures 1 and 2, this contrast between high- and low-water-content tissues persists over the entire radio frequency (RF) spectrum from power frequencies through millimeter waves.

Joines e*t al.* [5] measured to 0.9 GHz the ε_r, and σ of freshly excised tissues from the colon, kidney, liver, lung, breast, and muscle. Each tissue sample was taken from four to seven different patients, and each sample was measured at three different positions. Chaudhary *et al.*, [6] measured to 3GHz the ε_r, and σ of normal and malignant breast tissues obtained from 15 patients. The data of Joines *et al.*, at 0.9

GHz indicates that of malignant breast tumors exceeds that σ of normal breast tissue by 6.4: 1, and ε_r of malignant breast tumors exceeds that of normal breast tissue by 3.8: 1. Joines *et al.* further found that for breast tissues of the same type, the dielectric contrast between malignant and normal tissues is greatest for the mammary gland. The data of Chaudhary *et al.* up to 3 GHz indicate corresponding malignant tumor-to-normal breast tissue ratios of 4.7: 1 and 5: 1, in good agreement with Joines *et al.*

1.2.1 Malignant Tumor Properties

Foster and Schepps [7], Rogers *et al.* [8], and Peloso *et al.* [9] separately measured ε_r and σ of malignant tumors and found values above 1 GHz that are almost the same as for normal high-water-content tissues such as muscle. In some cases, ε_r and σ for malignant tumors were significantly greater than for normal muscle tissues, especially at frequencies below 1 GHz [10].

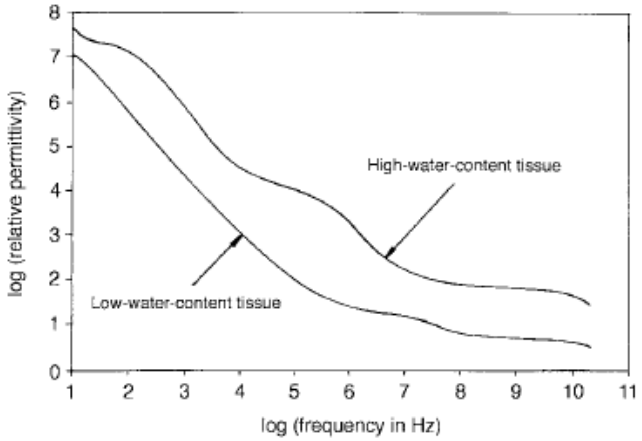

Figure 1: Comparison of the permittivity of high-water content tissue such as muscle with low- water content tissue such as fat as a function of frequency according to Gabriel et al

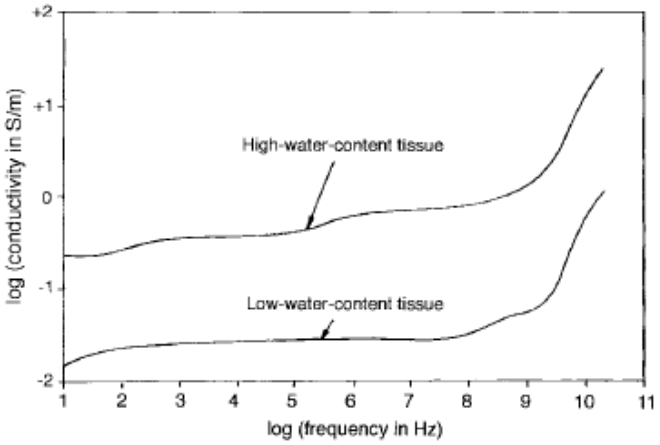

Figure 2: Comparison of the conductivity of high-water content tissue such as muscle with low- water content tissue such as fat as a function of frequency according to Gabriel et al.

Swarup *et al.* [10] studied the onset of the high values of ε_r and σ in malignant tumors by measuring MCA1 fibro sarcoma mouse tumors at 7, 15, and 30 days after inception. No significant variation of ε_r and σ was seen with tumor age. While the larger tumors exhibited a necrotic interior, they showed little difference in ε_r and σ above 0.5 GHz.

Surowiec *et al.* [11] performed measurements of cm-size malignant human breast tumors and adjacent tissues and found an increase in ε_r and σ of the normal breast tissue near malignant tumors. This effect may be caused by infiltration or vascularization. It could enlarge the microwave scattering cross-section and thereby aid in the confocal microwave detection of the tumor.

1.2.2 Skin and Veins

Gabriel *et al.* found that, for either wet or dry skin, $30 < \varepsilon_r < 40$ and $1 < \sigma < 10$ S/m from 1–10 GHz. While some dielectric property data exist for blood, none can be found for vein walls. For computational models, you can assume that the dielectric properties of a vein are the same as those of muscle.

1.2.3 Breast Geometry

The depth of a typical normal, non-lactating human breast is about 5 cm [12]–[14]. This suggests that a mildly compressed breast would span less than 5 cm between the skin surface and the rib cage. Further, almost 50% of all breast tumors occur in the quadrant near the armpit where the breast is less than about 2.5-cm deep.

1.3 Finite Difference Time Domain (FDTD)

The FDTD technique is used in solving electromagnetic scattering problem, because it can model an inhomogeneous object of arbitrary shape. It is a time domain numeric electromagnetic technique for solving Maxwell's equations. The Maxwell's equations are discretized in space and time. This is accomplished by mapping the volume of interest onto rectangular grid where the unknown field components are located in each cell. FDTD algorithm explicitly solves Maxwell's curl equations using central finite differences in both time and space. The FDTD grid is composed of rectangular boxes (called Yee cells). Each box edge is an electric field location, and the material for each mesh edge can be specified independently of other edges and each face is a magnetic field location. Assigning different materials to different mesh edges forms the geometry. Regular grid is chosen since making calculations for each grid is extremely fast. This allows precise approximations to the actual physical geometry.

FDTD method is a time stepping procedure. Inputs are time-sampled analog signals. By alternately calculating the electric and magnetic fields at each time step, fields are propagated throughout the mesh. The time-dependent differential form equations are given by,

$$\nabla \times E = -\frac{\delta B}{\delta t} \quad (1)$$

$$\nabla \times H = \frac{\delta D}{\delta t} + J \quad (2)$$

1.3.1 2-D FDTD Analysis of a Pulsed Microwave Confocal System for Breast Cancer Detection

1.3.2 Modeling of the Fixed Focus Elliptical System

As the first step in the systems analysis, a fixed focus confocal microwave system employing a metal elliptical reflector was computationally modeled in two dimensions using the finite-difference time-domain (FDTD) solution of Maxwell's equations, for the transverse magnetic case. The reflector was specified with one focal point at a monopole antenna element and one in a breast half-space 3.8 cm below the surface. (In such two-dimensional (2-D) models, all material structures in the computational space, including the antenna, are assumed to be infinitely long. Thus, there is no ground return for the antenna and it is termed a "monopole".

Figure 3 illustrates the FDTD model of this system. This model used a uniform grid with square unit cells as fine as 0.2 mm in the highest-resolution simulations. The reflector was assumed filled with lossless dielectric (ε_r = 9, σ = 0) matching the nominal breast permittivity, and was located at the surface of a half-space of normal breast tissue (ε_r = 9, σ = 0.4 S/m). No skin layer was modeled. The monopole antenna was excited by a 270-ps Gaussian pulse multiplying a 6-GHz sinusoid that passed through zero at the peak of the Gaussian. This signal has zero dc content and a Gaussian, double sideband (DSB) suppressed-carrier spectrum symmetric about 6 GHz. The full-width spectral bandwidth at half-maximum extends from 4 to 8 GHz. A circular tumor extends from 4 to 8 GHz. A circular tumor (ε_r = 50, σ = 7 S/m) was assumed located at the in-breast focus.

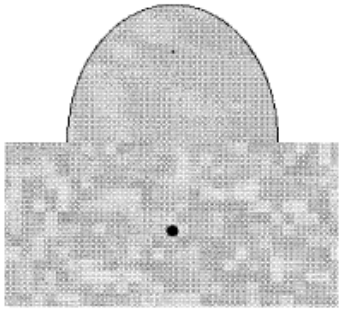

Figure 3: 2-D FDTD Computational model of the elliptical reflector system showing the heterogeneous breast tissue model and 0.5cm diameter tumor located at the in breast focus 3.8cm beneath the surface

1.3.3 ± 10% Random Heterogeneity of the Normal Breast Tissue

To simulate the heterogeneity of the normal breast tissue as measured by Joines *et al.* [5] and Chaudhary *et al.* [6], 10% random fluctuations of ε_r and σ were assigned to the breast tissue half-space in a checkerboard

pattern. Specifically, as shown in Fig.3, each square block of grid cells spanning 5×5mm was randomly assigned a value of ε_r and a value of σ in a 10% range centered about the nominal. This resulted in random, peak 20% jump discontinuities of the normal breast- tissue ε_r and σ at the scale of the tumor diameter. FDTD modeling was performed for a) no tumor present, to establish the background clutter; b) variable location of a tumor having a 0.5-cm fixed diameter; and c) variable diameter of a tumor having a fixed location at the in-breast focal point. The signal-to-clutter (S/C) ratio was obtained by comparing the peak backscattered responses of the heterogeneous breast model with and without the presence of the tumor.

Figure 4 depicts the calculated time waveforms of the backscattered power response for this model with and without the 0.5-cm-diameter tumor present at the in-breast focus 3.8 cm below the surface. Upon forming the ratio of the peak back scattered pulse amplitude with the tumor present to the peak back scattered pulse amplitude without the tumor present, the S/C ratio is found to be 12dB. Figure 5 graphs the calculated S/C for the 0.5-cm diameter tumor as a function of the tumor's lateral position from the focus for a constant depth of 3.8 cm. We infer from this figure that the lateral resolution in locating the tumor in the presence of the clutter is about 0.5 cm. Figure 6 graphs the calculated S/C for a tumor fixed in position at the in-breast focus as a function of the tumor's size. We infer from this figure that tumors having diameters as small as 0.2 cm can yield responses that are 12 dB above the background clutter due to the random ±10% tissue heterogeneity.

1.3.4 ± 20% Random Heterogeneity of the Normal Breast Tissue

The above study was repeated for an increased heterogeneity of the normal breast tissue of ± 20% about the nominal, more than twice which experimentally was observed by Joines *et al.* [5] and Chaudhary *et al.* [6]. This resulted in random, peak ±40% jump discontinuities of the normal-breast-tissue ε_r and σ at the scale of the tumor diameter. While the computed S/C ratios were reduced by 5–6 dB relative to the ±10% heterogeneity case, the S/C remained greater than 6 dB for tumor diameters of 0.2 cm or larger. Further, the systems lateral resolution was unchanged (about 0.5cm).

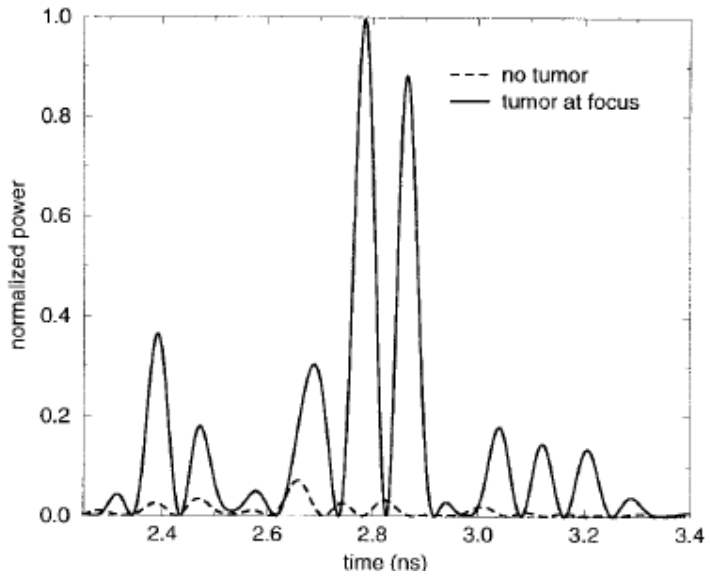

Figure 4: FDTD-computed time domain waveforms of the backscattered response with and without the 0.5cm diameter tumor present at the in-breast focus

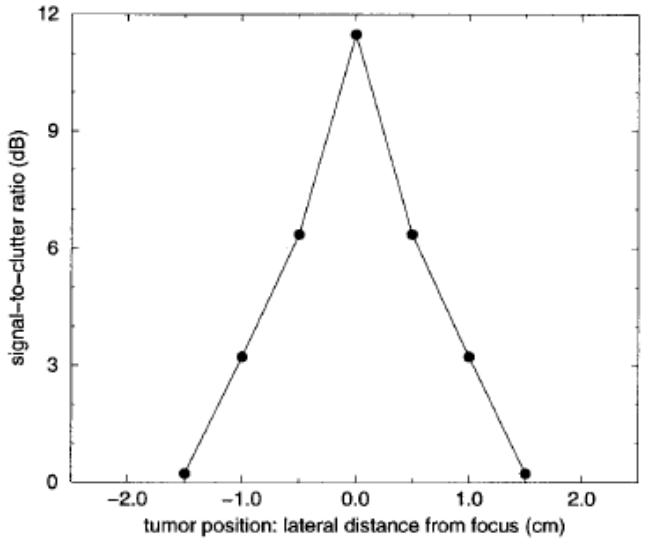

Figure 5: Signal to clutter (S/C) ratio for the back scattered response of the 0.5cm diameter tumor as a function of the tumor's lateral distance from the in-breast focus

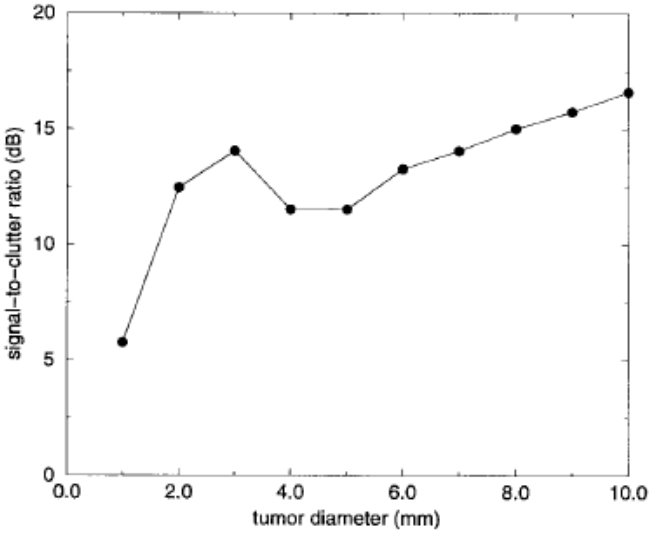

Figure 6: Signal to clutter (S/C) ratio for the backscattered response of a tumor at the in-breast focus as a function of tumor's size

1.4 Finite Volume Time Domain

The Finite-Volume Time-Domain (FVTD) method, as a general time-domain field solver, has successfully been applied to a variety of electromagnetic structures. The advantage of an unstructured mesh with tetrahedral volume elements places the FVTD method somewhat in between the Finite Element Time-Domain (FETD) method and the Finite-Difference Time- Domain (FDTD) method. Since the FVTD method is still in its infancy in computational electromagnetic application – at least in comparison to the FDTD method – the potential of this relatively new approach has not been fully unfolded yet. Although several authors have illustrated the capability of the FVTD method for the analysis of large scale problems [15] or problems with fine details surrounded by curved linear boundaries [16], the achievable accuracy for the FVTD method in particular for problems requiring a large dynamic range, has not been demonstrated so far. The FVTD method is inherently

applied in unstructured meshes and thus is able to approximate complex geometries naturally without additional effort. In contrast, methods using structured meshes, e.g. a classic stair casing FDTD approach, may need to incorporate artificial treatment of boundaries to meet certain accuracy requirements.

1.4.1 Electromagnetic Wave Diffraction using a Finite Volume Method

Simulation of near fields scattered by an aircraft illuminated by an incident plane wave will be discussed. An exciting Gaussian pulse in the time domain is used for the following example in the computational time interval. The scatterer is assumed to be perfectly conductive. In Figs. 7 and 8, we present the meshes used for the numerical simulations. For the FDTD, the computational domain is composed of 4144000 volumes and for FVTD, the discretization leads to 79361 volumes with the same minimum mesh size. The results presented in Fig. 9 shows the x-component of the electric field and the y-component of the magnetic field computed at points A and B with the two methods. In this example the use of FVTD permits an important gain in memory and a gain of 3 in time compared with FDTD, despite a smaller time step to ensure the scheme's stability and a larger number of operations in FVTD than in FDTD.

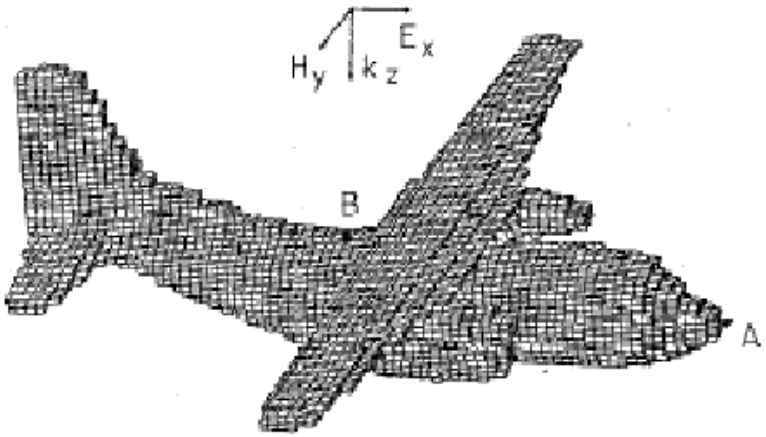

Figure 7: FDTD meshing

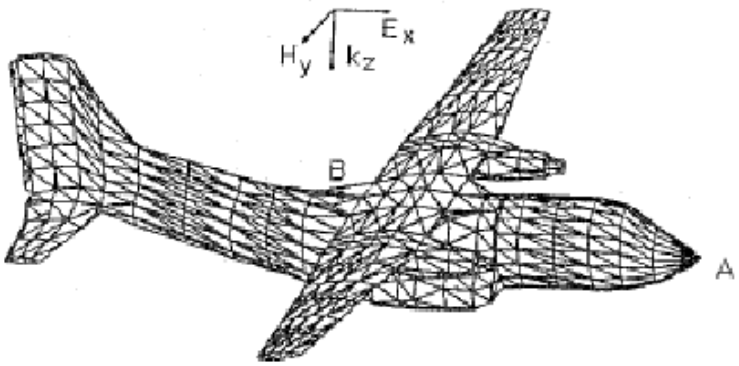

Figure 8: FVTD meshing

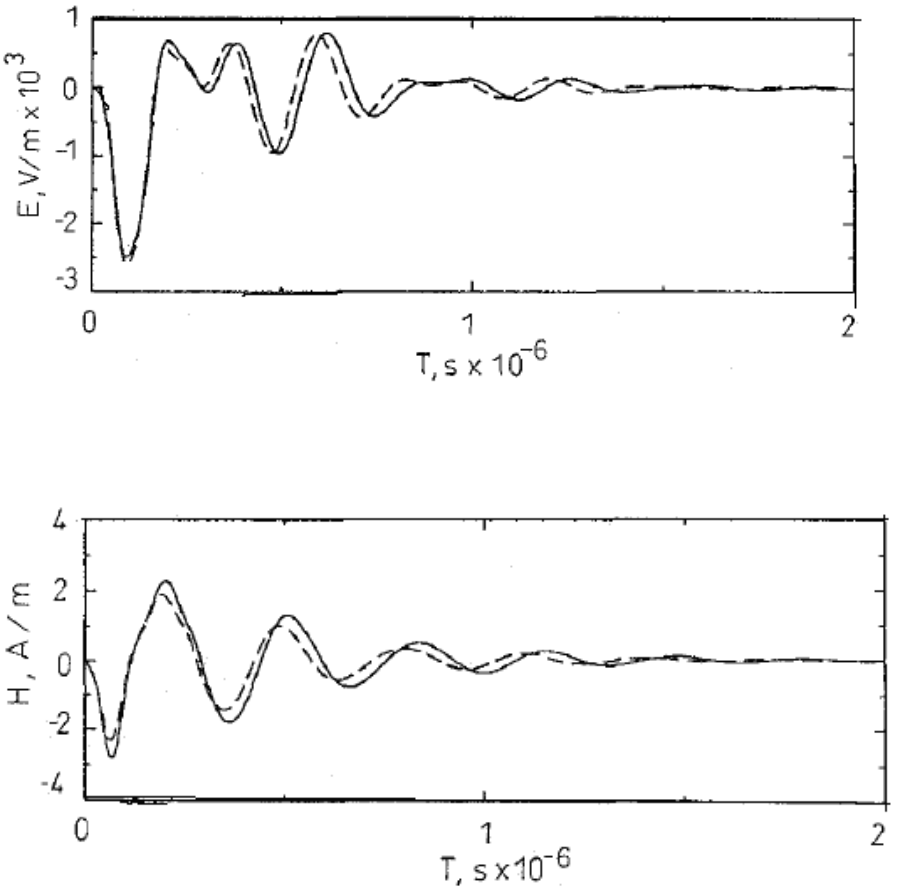

Figure 9: Comparison between FDTD and FVTD

1.5 Conclusion

The finite volume technique seems to be an interesting approach for the study of electromagnetic wave diffraction. Scatterers with 'complex' surfaces can be treated. The higher computational time required in FVTD can be compensated by a conformal unstructured meshing of the objects allowing local refinement mesh easier than in FDTD. Moreover with the finite volume scheme, thin material with finite conductivity and dielectric part can be taken into account easily.

References

Gabriel, C. (1996). "A compilation of the dielectric properties of body tissues at RF and microwave frequencies," Radiofrequency Radiation Division, Brooks AFB, San Antonio, TX, Contract AL/OE TR-1996-0037.

Gabriel, C., Gabriel, S. and Corthout, E. (1996). "The dielectric properties of biological tissues: I. Literature survey," *Phys. Med., Biol.,* **41**(11), pp. 2231–2249.

Gabriel, S., Lau, R. W. and Gabriel, C. (1996). "The dielectric properties of biological tissues: II. Measurements on the frequency range 10 Hz to 20 GHz," *Phys. Med., Biol.,* **41**(11), pp. 2251 2269.

Joines, Y. Z. Dhenxing and Jirtle, R. L. (1994). "The measured electrical properties of normal and malignant human tissues from 50 to 900 MHz," *Med. Phys.,* **21**, pp. 547–550.

Chaudhary, S. S., Mishra, R. K., Swarup A. and Thomas, J. M. (1984). "Dielectric properties of normal and malignant human breast tissues at radiowave and microwave frequencies," *Indian J. Biochem., Biophys.,* vol. **21**, pp. 76–79.

Foster, K. R. and Schepps, J. L. (1981). "Dielectric properties of tumor and normal tissue at radio through microwave frequency," *J. Microwave Power,* vol. **16**, pp. 107–119.

Rogers, J. A., Shepard, R. J., Grant, E. H., Bleehen, N. M. and Honess, D. J. (19830. "The dielectric properties of normal and tumor mouse tissue between 50 MHz and 10 GHz," *Br. J. Radiol.,* vol. **56**, pp. 335-338.

Peloso, R., Tuma, D. and Jain, R. K. (1984). "Dielectric properties of solid tumors during normothermia and hyperthermia," *IEEE Trans. Biomed.Eng.,* vol. BME-31, pp. 725–728.

Swarup, S., Stuchly, S. S. and Surowiec, A. (1991). "Dielectric properties of mouse MCA1 fibro sarcoma at different stages of development," *Bioelectromagn.,* vol. **12**, pp. 1–8.

Surowiec, A. J., Stuchly, S. S., Barr J. R. and Swarup A. (1988). "Dielectric properties of breast carcinoma and the surrounding tissues," *IEEE Trans. Biomed. Eng.,* vol. **35**, pp. 257–263.

Gray, H. Anatomy of the Human Body, C. M. Goss, Ed. Philadelphia, PA: Lea and Febiger, 1949.

Wu, X., Barnes, G. T. and Tucker, D. M. (1991). "Spectral dependence of glandular tissue dose in screen-film mammography, Radiol" vol. **179**, pp. 143–148.

Rosenstein, M., Andersen, L. W. and Warner, G. (1985). "Handbook of glandular tissue doses in mammography," U.S. Government Printing Office, Washington, DC, HHS (FDA) Publication 858239.

Bonnet, P., Ferrieres, X., Paladian, F., Grando, J., Alliot, J. and Fontaine, J. (1997). "Electromagnetic wave diffraction using a finite volume method," *IEE Electr. Letters*, vol. **33**(1), pp. 31–32.

Fumeaux, C., Baumann, D. and Vahldieck, R. (204). "Advanced FVTD simulations of dielectric resonator antennas and feed structures," *ACES Journal*, vol. **19**(3), pp. 155–164.